Oxid Met (2013) 79:41–51
DOI 10.1007/s11085-012-9354-y

ORIGINAL PAPER

Development of Oxide Scale at 1,100 °C on Fe20Cr5Al Alloy Non-Implanted and Yttrium-Implanted

Jerzy Jedliński · Jean-Luc Grosseau-Poussard · Kazimierz Kowalski · Jarosław Dąbek · Günter Borchardt

Received: 22 June 2012 / Published online: 4 January 2013

Abstract The development of the oxide scale on model Fe20Cr5Al-type alloys unmodified and containing implanted yttrium was studied in oxygen-dominated atmosphere at 1,100 °C for up to 1 h. A two-stage-oxidation exposure was applied with the use of $^{18}O_2$ as a tracer. The choice of the exposure durations ensured the possibility to follow the consecutive stages of scale development. The oxidized samples were characterized using SEM (morphology); PLS (phase composition), and SIMS (elemental distributions). The obtained results are discussed in terms of the mechanism of the development of protective α-Al_2O_3 scale and the effect of the additions on this process taking into account the necessity of distinguishing the

J. Jedliński (✉)
Surface Engineering and Analysis Lab, Department of Solid State Chemistry and Modelling of Processes, Faculty of Materials Science and Ceramics, AGH University of Science and Technology, al. Mickiewicza 30, 30-059 Kraków, Poland
e-mail: jedlinsk@agh.edu.pl

J.-L. Grosseau-Poussard
LaSIE, Université de La Rochelle, Avenue Michel Crépeau Fermi, 17042 Cedex 01, France
e-mail: jlgrouss@univ-lr.fr

K. Kowalski
Faculty of Metal Engineering and Industrial Computer Science, AGH University of Science and Technology, al. Mickiewicza 30, 30-059 Kraków, Poland
e-mail: kazimierz.kowalski@agh.edu.pl

J. Dąbek
Department of Solid State Chemistry and Modelling of Processes, Faculty of Materials Science and Ceramics, AGH University of Science and Technology, al. Mickiewicza 30, 30-059 Kraków, Poland
e-mail: dabek@agh.edu.pl

G. Borchardt
Clausthaler Zentrum für Materialtechnik, Technische Universität Clausthal, Agricolastr. 2, 3392 Clausthal-Zellerfeld, Germany
e-mail: Guenter.Borchardt@tu-clausthal.de

mechanism and kinetics of the scale evolution. Similar scale evolution stages were found on both studied materials and in both cases the protective α-Al_2O_3 scale developed rapidly, already after the exposure for 3 min. Implanted yttrium appeared to have a negligible effect on the evolution of the scale. It only slightly retarded the evolution which can be attributed rather to a kinetic effect than to mechanistic one. However, the mechanical failure of the scales via formation of cracks at the asperities of convolutions occurred on the yttrium-implanted alloy but not on the non-implanted one.

Keywords FeCrAl high temperature alloys · Reactive elements · Alumina scales

Introduction

FeCrAl-type alloys containing reactive elements (Y, Hf, Zr, …) constitute one of the best metallic materials for high temperature ($T \geq 900$ °C) applications in oxidizing atmospheres. Although it was observed that the formation of the protective α-Al_2O_3 scale at temperatures 1,000 °C and higher is relatively rapid [1, 2], this process was not studied in detail, so far and, therefore, it is still necessary to verify this view at various temperatures in order to predict the behavior of these alloys in terms of their response to service conditions, in particular to thermal cycling. The presence of transient aluminium oxides (γ-, δ- and/or θ-Al_2O_3) may be important for two following reasons: (i) their transformation into α-Al_2O_3 is accompanied by ca. 10 % volume contraction causing tensile stresses the relief of which can bring about mechanical failure of the scales through cracking; and (ii) in complex scales, having multilayered microstructure or exhibiting regions with different phase composition, comprising both types of alumina phases, transient and alpha, mechanical failure can occur during temperature changes due to the different thermal expansion coefficients of components.

This paper is focused on the early oxidation of Fe20Cr5Al alloy at 1,100 °C and the effect of implanted Yttrium addition. The applied systematic approach relies on the particular choice of the exposure conditions and following the consecutive stages of the scale evolution in terms of its morphology, phase composition and growth mechanism.

Ion implantation was applied as the way of introduction of Yttrium for two following reasons: (i) it enables incorporation of the addition in a fairly controlled way; and (ii) it offers similar benefits concerning the scale resistance to spallation to the alloyed Yttrium for limited but still reasonable oxidation periods (i.e. [3]). Therefore, it is a useful tool to study the effect of additions on the oxidation behavior of alumina and chromia formers.

Experimental Procedures

The synthetic Fe20Cr5Al alloy was manufactured by INCO company (courtesy of Prof. W. J. Quadakkers, Forschungszentrum Jülich, Germany) using conventional

melting. Standard sample preparation procedure resulted in ca. 1-mm thick discs, polished down to the 1-μm diamond paste. Subsequently, discs were ultrasonically degreased in acetone. Yttrium was implanted into the surface layer of some specimens or of their parts, the remaining part being left unmodified. The following implantation parameters were used: ion beam energy of 70 keV and dose of 2×10^{16} ions/cm^2. The enrichments in implanted additions were calculated according to the LSS-theory [4], to be less than 35 nm. The concentration maximum of the assumed Gauss distribution was at the depth of ca. 16 nm, and it was ca. 7 at.%. The exact data cannot be obtained using SIMS measurements because this technique is only semi-quantitative, as described elsewhere [5].

A series of two-stage-oxidation exposure in which the $^{18}O_2$ was used as a tracer was carried out at 1,100 °C. The procedure that has been described elsewhere [5] was systematic in that the duration of the first stage of each subsequent experiment was equal to the total duration of the previous experiment. The exposure periods were following: (i) 2 min in $^{16}O_2$ followed by 1 min in $^{18}O_2$; (ii) 3 min in $^{16}O_2$ followed by 4 min in $^{18}O_2$; (iii) 7 min in $^{16}O_2$ followed by 8 min in $^{18}O_2$; and (iv) 15 min in $^{16}O_2$ followed by 45 min in $^{18}O_2$. Thus, the exposure period from 3 min to 1 h was covered in four experiments.

The scales were characterized by means of the scanning electron microscopy (SEM) to observe the surface morphology of the scales, the photo-stimulated luminescence spectroscopy (PLS, lateral resolution down to 1 μm) to determine the phase composition of the scales, and a high-spatial-resolution secondary ion mass spectrometry (HSR-SIMS, spatial resolution of ca 0.5 μm) to determine the elemental distribution profiles across the scales. The oxygen isotopic (^{16}O and ^{18}O) profiles were normalized which resulted in their relative in-depth distribution profiles necessary for inferring information concerning the scale growth mechanism. The whole procedure and the rules concerning the interpretation of these results were described in detail elsewhere [3]. In all HSR-SIMS analyses the regions of the shape of squares of size 29 × 29 μm were chosen which are representative for the whole surface of the scale. It means that similar results were obtained using smaller size of the analyzed regions. The PLS results were interpreted in terms of referring to the literature data [6]. The additional PLS analyses were carried out, with the reduced wavelength range in order to enable detection of θ-Al_2O_3-related doublet which otherwise was too low to be observed together with that of α-Al_2O_3-related one.

Results

The results are shown in Figs. 1, 2, 3, 4, 5, 6, 7 and 8 in terms of the surface view of the scales, the PLS spectra, and relative distribution of oxygen isotopes across the scales growing on non-implanted (Figs. 1, 2, 3, 4) and Yttrium-implanted (Figs. 5, 6, 7, 8) alloys. The distribution profiles of positive ions across the scales formed on Yttrium-implanted alloy are shown for various exposure periods in Fig. 9 mainly in order to determine the distribution of Yttrium.

On non-implanted alloy initially, after 3 min of oxidation, the scale exhibits slightly irregular surface morphology (Fig. 1a) and a combination of outward and

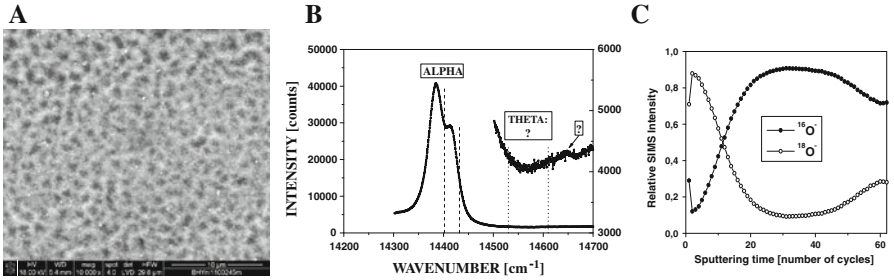

Fig. 1 Surface of the scale (**a**) formed on non-implanted Fe20Cr5Al alloy oxidized at 1,100 °C for 3 min (2 min in $^{16}O_2$ followed by 1 min in $^{18}O_2$-rich atmosphere), the corresponding PLS spectrum (**b**), and the SIMS-profiles of the relative distribution of oxygen isotopes (**c**) across the scale

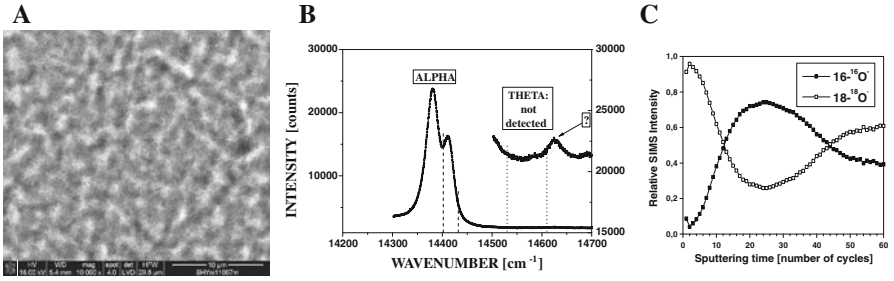

Fig. 2 Surface of the scale (**a**) formed on non-implanted Fe20Cr5Al alloy oxidized at 1,100 °C for 7 min (3 min in $^{16}O_2$ followed by 4 min in $^{18}O_2$-rich atmosphere), the corresponding PLS spectrum (**b**), and the SIMS-profiles of the relative distribution of oxygen isotopes (**c**) across the scale

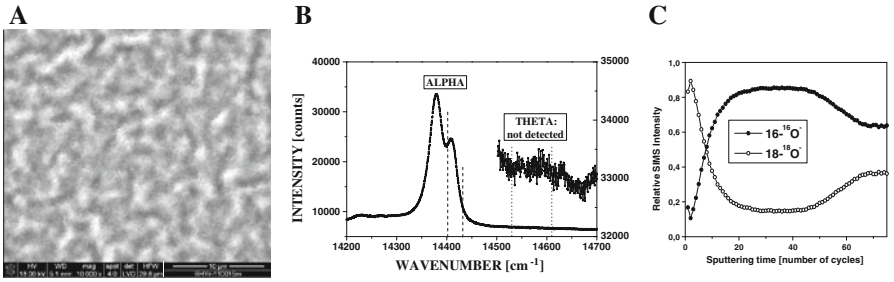

Fig. 3 Surface of the scale (**a**) formed on non-implanted Fe20Cr5Al alloy oxidized at 1,100 °C for 15 min (7 min in $^{16}O_2$ followed by 8 min in $^{18}O_2$-rich atmosphere), the corresponding PLS spectrum (**b**), and the SIMS-profiles of the relative distribution of oxygen isotopes (**c**) across the scale

inward growth mechanism, the former of which prevails (Fig. 1c). This scale consists essentially of α-Al_2O_3 (Fig. 1b). A very little doubt concerns the absence of θ-Al_2O_3: even for extended period of PLS-data acquisition, twenty times of that applied to observe the α-related doublet, the luminescence associated with the wavelength corresponding to θ-related maximum does not appear as distinct enough (right-hand side of Fig. 1b). This part of the PLS spectrum contains one maximum

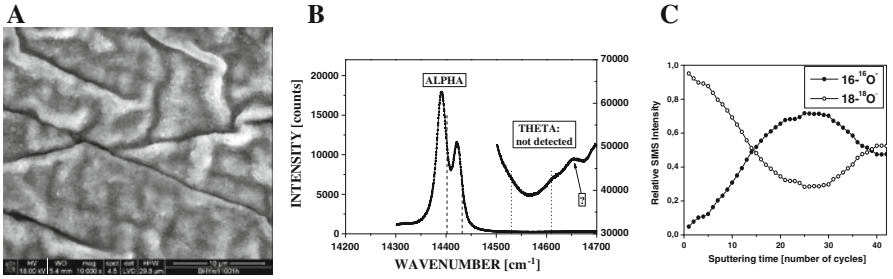

Fig. 4 Surface of the scale (**a**) formed on non-implanted Fe20Cr5Al alloy oxidized at 1,100 °C for 1 h (15 min in $^{16}O_2$ followed by 45 min in $^{18}O_2$-rich atmosphere), the corresponding PLS spectrum (**b**), and the SIMS-profiles of the relative distribution of oxygen isotopes (**c**) across the scale

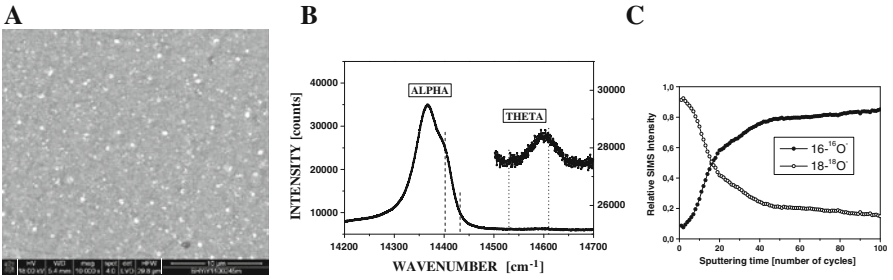

Fig. 5 Surface of the scale (**a**) formed on Yttrium-implanted Fe20Cr5Al alloy oxidized at 1,100 °C for 3 min (2 min in $^{16}O_2$ followed by 1 min in $^{18}O_2$-rich atmosphere), the corresponding PLS spectrum (**b**), and the SIMS-profiles of the relative distribution of oxygen isotopes (**c**) across the scale

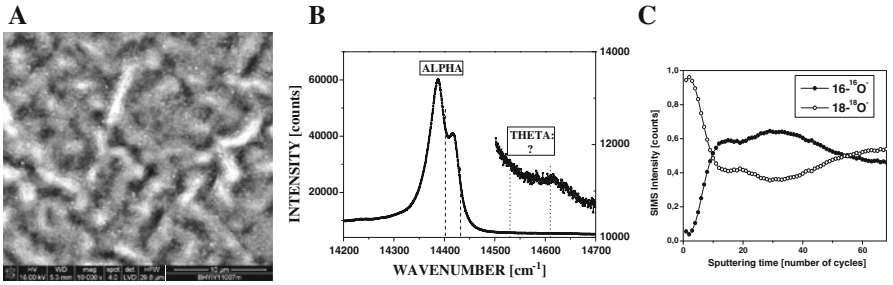

Fig. 6 Surface of the scale (**a**) formed on Yttrium-implanted Fe20Cr5Al alloy oxidized at 1,100 °C for 7 min (3 min in $^{16}O_2$ followed by 4 min in $^{18}O_2$-rich atmosphere), the corresponding PLS spectrum (**b**), and the SIMS-profiles of the relative distribution of oxygen isotopes (**c**) across the scale

which cannot be unambiguously defined (question mark in Fig. 1c) which also is observed in some other cases (Figs. 4b, 7b, 8b). Prolonged oxidation brings about: (i) further development of irregularities which successively form the 'wavy'-type of morphology, usually referred to as convoluted [7] or wrinkled [8], (ii) substantial increase of the inward growth mechanism component (Figs. 2, 3, 4a and c,

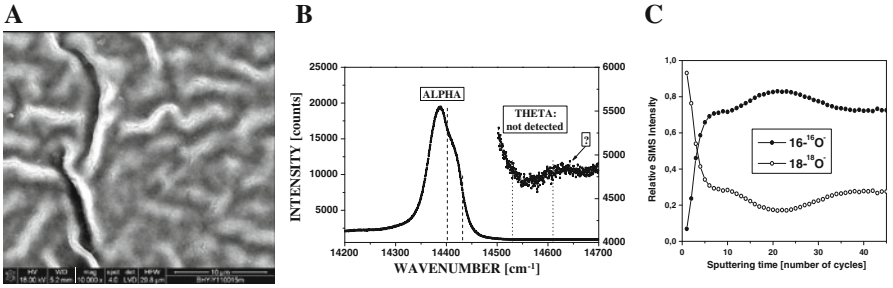

Fig. 7 Surface of the scale (**a**) formed on Yttrium-implanted Fe20Cr5Al alloy oxidized at 1,100 °C for 15 min (7 min in $^{16}O_2$ followed by 8 min in $^{18}O_2$-rich atmosphere), the corresponding PLS spectrum (**b**), and the SIMS-profiles of the relative distribution of oxygen isotopes (**c**) across the scale

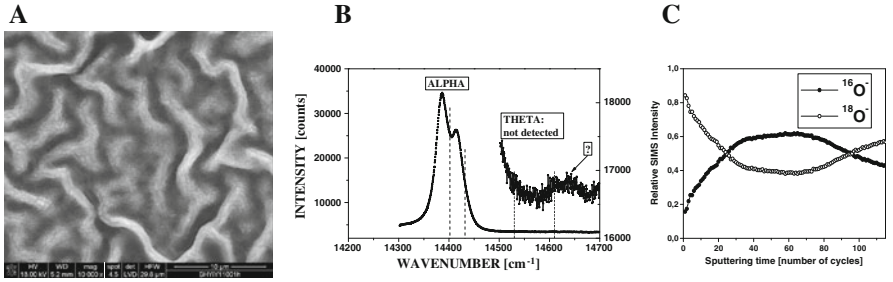

Fig. 8 Surface of the scale (**a**) formed on Yttrium-implanted Fe20Cr5Al alloy oxidized at 1,100 °C for 1 h (15 min in $^{16}O_2$ followed by 45 min in $^{18}O_2$-rich atmosphere), the corresponding PLS spectrum (**b**), and the SIMS-profiles of the relative distribution of oxygen isotopes (**c**) across the scale

respectively). For all the exposure times from 7 min to 1 h, the only detected oxide phase in the scale is α-Al_2O_3 (Figs. 2b, 3b, 4b).

On Yttrium-implanted alloy the shortest oxidation, of duration of 3 min, leads to rather regular surface morphology of the scale (Fig. 5a) and a predominant outward growth mechanism (Fig. 5c). However, the relatively large SIMS intensity of the signal from ^{18}O oxygen tracer observed after sputtering of the scale and exposing its deeper regions towards the scale-substrate interface, indicates the possible inward growth mechanism component.

From the main curve of the PLS analysis only α-Al_2O_3 can be detected (Fig. 5b). However, the complementary spectrum clearly shows maximum corresponding to θ-Al_2O_3 (right-hand curve in Fig. 5b) which is too low to be detected together with that of α-Al_2O_3. The minor presence of θ-phase can be inferred from right-hand curve in Fig. 6b which corresponds to the scale formed after 7 min oxidation but not for the more prolonged exposures (Figs. 7b, 8b). In all these cases, α-phase predominates. Similar features of scale morphology (development of convoluted morphology) and growth mechanism (increase of the inward component) after prolonged oxidation, 7 min to 1 h, to mentioned above observed on non-implanted alloy concern also the scales on Yttrium-implanted one (Figs. 6, 7, 8a and c).

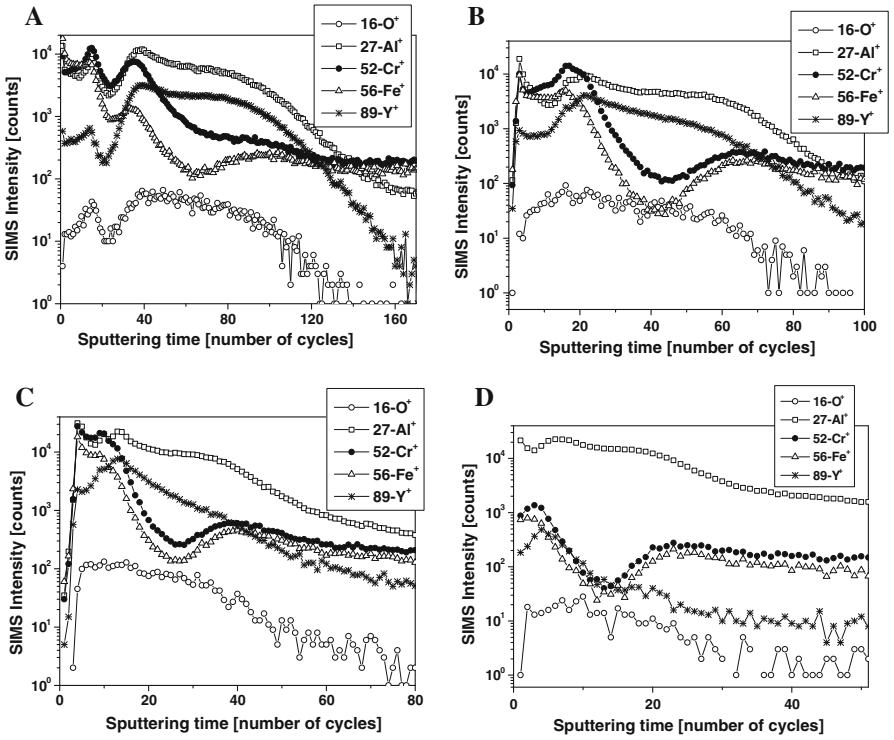

Fig. 9 SIMS distribution profiles of the positive ions across the scales formed on Yttrium-implanted Fe20Cr5Al alloy oxidized at 1,100 °C for: **a** 3 min, **b** 7 min, **c** 15 min, **d** 1 h

However, three following differences should be noticed: (i) the more convoluted scale morphology develops on Y-implanted alloy; (ii) frequently, the fine cracks are observed at asperities of wrinkles in scales on Y-implanted alloy but not on non-implanted one, as illustrated additionally in Fig. 10; (iii) on Y-implanted alloy the relatively high SIMS-intensity of the ^{18}O tracer is observed across the whole scale and not only at scale-gas and scale-substrate interfaces. Moreover, in some cases in the α-Al_2O_3-related PLS signal its doublet shape cannot be easily distinguished (Figs. 5b, 7b).

Concerning the SIMS distribution profiles of positive ions the following can be inferred (Fig. 9): (i) Yttrium, implanted prior to oxidation, incorporates significantly into the scale and its relative SIMS-intensity successively decreases with increased oxidation time and, consequently, the scale thickness; (ii) irregular shape of the distribution profiles is observed at the outermost part of the scale; (iii) Yttrium-related SIMS-intensity is significantly lower in this outermost scale layer, the majority of it being observed beneath this layer with highest intensity just at the border between the outermost layer and the remaining part of the scale; (iv) the relative SIMS intensity of iron and chromium ions with respect to that of aluminium

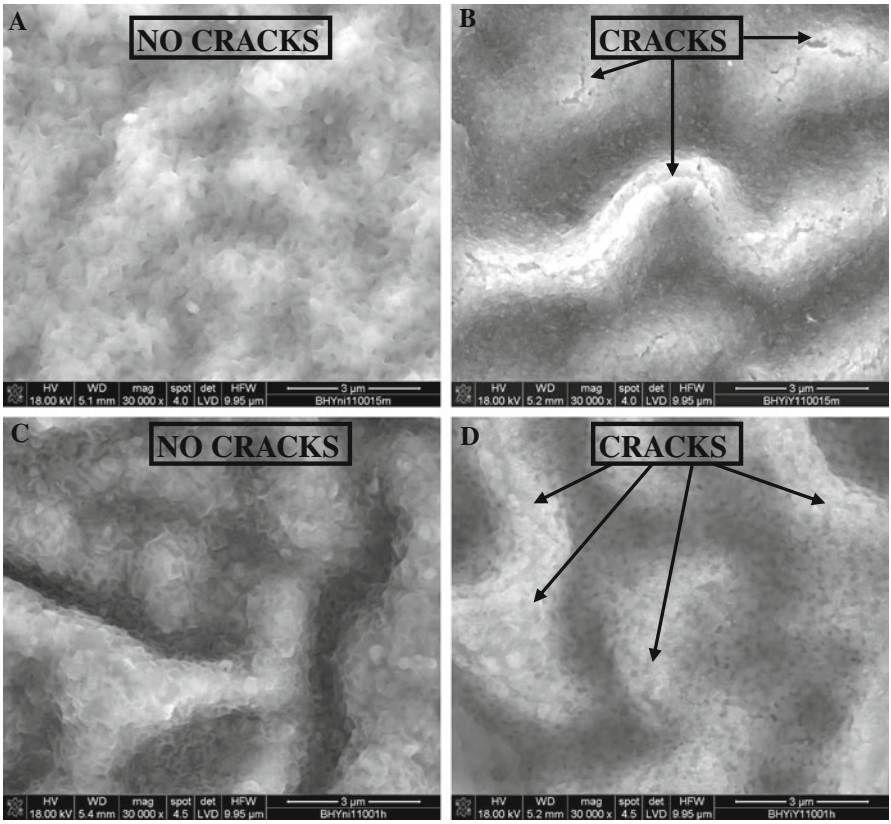

Fig. 10 Convoluted scales on non-implanted (**a**, **c**) and Yttrium-implanted (**b**, **d**) Fe20Cr5Al alloy oxidized at 1,100 °C for: **a, b** 15 min, **c**, **d** 1 h

ions is significant in the whole scale formed during oxidation for up to 15 min and the highest in the mentioned above outermost layer.

Discussion

The following should be mentioned concerning the applied methods:

(i) the probing depth of PLS was sufficient to obtain the signal from the whole scale because the scales formed under studied conditions were rather thin, having thicknesses not exceeding 1 μm;

(ii) the maxima from the α-Al_2O_3 doublet were shifted with respect to these given in the literature and marked using vertical dotted lines in Figs. 1b, 2b, 3b, 4b, 5b, 6b, 7b and 8b, because of the strains resulted from stresses generated in the scale related to the volume contraction during the phase transformation of transient aluminium oxides (γ, δ, and/or θ) into α-phase and compressive

stresses in α-Al_2O_3 during its further growth and cooling, as described elsewhere [9, 10];

(iii) the lack of distinct doublets in PLS spectra may result from contribution of different grains to the signal. It happens if the probed size is larger than grain size of the target or if few grains appear across the scale. Alternatively, the stress gradient across the scale can cause such an effect;

(iv) instability of SIMS intensity appears from the beginning of the analysis till the sputtering conditions are stable [3] which results in low reliability of the results in this range of sputtering time. However, it usually takes only few sputter cycles and, therefore, does not affect the interpretation of the reported results;

(v) the so-called 'matrix-effect' during the SIMS in-depth profiling occurs which manifests itself in dependence of sputtering rate on the target composition, microstructure and/or structure, as described elsewhere [5]. Therefore, for multilayered targets, considerably different SIMS-intensities can be obtained from various layers, with strong changes at the interfacial regions. This effect was observed in Fig. 9a–c at the outermost layer of the scale.

The obtained results indicate that at studied temperature, 1,100 °C, the scale evolution on both, non-implanted and Yttrium-implanted alloys occurs in a similar way in terms of its morphology, phase composition and growth mechanism. Only minor differences were observed. Rapidly, the scale morphology became convoluted, and inward component contributed substantially to the overall growth mechanism. No morphology features observed typically at lower temperatures, as blade-like grains and/or pyramids [1, 2, 11] were found. However, from all the SIMS relative distribution profiles of oxygen isotopes it appears also the outward component. In order to interpret this result it should be noted that the following processes contribute to the outward growth mechanism [12]: (i) the outward metal transport in transient aluminium oxides as well as in iron and/or chromium oxides, and (ii) the possible 'dislocation climbing' mechanism at the grain boundaries of α-Al_2O_3 [13]. Because the latter was practically the only phase present in the scale, it appears that the second explanation is the case in this study.

One of the most important conclusions is that even as short oxidation as for 3 min is sufficient to result in formation of the protective scale comprising α-Al_2O_3. This finding quantitatively indicates that the phase transformation of transient aluminium oxides into α-phase has occurred during initial 3 min of oxidation and that for FeCrAl alloys oxidized at 1,100 °C transient oxidation stages are extremely short. Therefore, the substrate protection by the α-Al_2O_3 oxide layer is efficient practically from the beginning of the reaction.

Implanted Yttrium appeared to retard slightly the evolution rate of the scale, but its effect was negligible. It manifested itself in flat scale instead of convoluted one after oxidation for 3 min (Fig. 5a) and, simultaneously, less pronounced inward growth mechanism (Fig. 5c) as well as in the presence of small amounts of θ-Al_2O_3 in the scale (Figs. 5b, 6b). However, it brought about rather more convoluted scale morphology and its mechanical failure at the asperities of wrinkles (cracks in Fig. 10b, d) which should be considered as detrimental effect.

The relatively high SIMS-intensity of the ^{18}O tracer observed across the whole scale on Yttrium-implanted alloy (Figs. 6c, 7c, 8c) can be attributed to the inward penetration of oxygen via mentioned above cracks the small size and high surface fraction of which make the overall process efficient. An alternative explanation would be related to the effective inward grain boundary oxygen diffusion across the α-Al_2O_3 scale. In such case the grain size of the scale should be smaller than that of the scale on non-implanted alloy. This explanation cannot be verified basing on the experiments carried out and requires further study.

Two following comments should be added concerning the interpretation of the results: (i) the protectiveness offered by the α-Al_2O_3 is activated as soon as it forms a continuous sub-layer of the scale even if transient aluminium oxides are still present but not across the entire scale; and (ii) distinguishing between the mechanistic and kinetic effects of Yttrium on the scale evolution relies on how it affects the consecutive stages of the evolution. Concerning the latter, mechanistic effects rely on affecting the sequence of consecutive stages, independent of the rate of their development, while the latter effects rely on affecting the rate of the evolution in terms of when the consecutive stages occur under given exposure conditions (temperature, atmosphere, regime).

Concluding Remarks

The systematic study of the development of the oxide scale on non-implanted and Yttrium-implanted Fe20Cr5Al alloy at 1,100 °C for period ranging from 3 min to 1 h led to the following conclusions:

1. A combination of series of two-stage-oxidation exposures and SEM, PLS and SIMS analytical tools is an useful approach to study the evolving oxide scales on alumina formers;
2. The scale evolution occurs via similar stages on both studied materials;
3. The protective α-Al_2O_3 scale develops rapidly, already after the exposure for 3 min on both alloys;
4. Convoluted scales successively appear and are observed after the oxidation for 7 min;
5. Implanted Yttrium exhibits negligible effect on the evolution of the scales, only slightly retarding it: it is rather kinetic effect than mechanistic one;
6. Mechanical failure of the scales via formation of cracks at the asperities of convolutions occurs on Yttrium-implanted alloy but not on non-implanted one;
7. A self-consistent interpretation of the growth mechanism investigation using $^{18}O_2$ tracer and SIMS requires careful approach in which the scale phase composition, morphology and microstructure were taken into account.

Acknowledgments The authors would like to acknowledge gratefully the Region Poitou–Charentes, France and AGH University of Science and Technology, Kraków, Poland for financial support.

References

1. S. Chevalier, A. Galerie, O. Heintz, R. Chassagnon, and A. Crisci, *Materials Science Forum* **595–598**, 915 (2008).
2. J. Jedlinski, J. L. Grosseau-Poussard, M. Nocuń, G. Smoła, K. Kowalski, J. Dąbek, A. Rakowska, and G. Bonnet, *Materials Science Forum* **696**, 70 (2011).
3. J. Jedlinski, *Solid State Ionics* **101–103**, 1033 (1997).
4. J. Lindhard, M. Scharff, and H. Schiott, *Matematisk-Fysiske Meddelelser Danske Videnskabernes Selskab* **33**, 1 (1963).
5. J. Jedlinski, A. Bernasik, K. Kowalski, and M. Nocun, *Materials at High Temperatures* **12**, 505 (2005).
6. D. M. Lipkin and D. R. Clarke, *Oxidation of Metals* **45**, 267 (1996).
7. F. A. Golightly, F. H. Stott, and G. C. Wood, *Oxidation of Metals* **10**, 163 (1976).
8. V. K. Tolpygo and D. R. Clarke, *Acta Materialia* **46**, 5153 (1998).
9. R. J. Christensen, D. M. Lipkin, and D. R. Clarke, *Applied Physics Letters* **69**, 3754 (1996).
10. R. J. Christensen, V. K. Tolpygo, and D. R. Clarke, *Acta Materialia* **45**, 1761 (1997).
11. H. El-Kadiri, R. Molins, Y. Bienvenu, and M. F. Horstemeyer, *Oxidation of Metals* **64**, 63 (2005).
12. J. Jedlinski, *Defect and Diffusion Forum* **289–292**, 385 (2009).
13. D. R. Clarke, *Acta Materialia* **51**, 1393 (2003).